Low T dynamical properties of spin glasses smoothly extrapolate to $T = 0$

2002 J. Phys. A: Math. Gen. 35 6805

(http://iopscience.iop.org/0305-4470/35/32/303)

INSTITUTE OF PHYSICS PUBLISHING JOURNAL OF PHYSICS A: MATHEMATICAL AND GENERAL

J. Phys. A: Math. Gen. **35** (2002) 6805–6814 PII: S0305-4470(02)35200-4

Low T dynamical properties of spin glasses smoothly extrapolate to $T = 0$

Enzo Marinari[1], Giorgio Parisi[1] and Juan J Ruiz-Lorenzo[2]

[1] Dipartimento di Fisica, SMC and UdR1 of INFM and INFN, Università di Roma, 'La Sapienza', P A Moro 2, 00185 Roma, Italy
[2] Departamento de Física, Facultad de Ciencias, Universidad de Extremadura, E-06071 Badajoz, Spain

E-mail: enzo.marinari@roma1.infn.it, giorgio.parisi@roma1.infn.it and ruiz@unex.es

Received 26 March 2002
Published 2 August 2002
Online at stacks.iop.org/JPhysA/35/6805

Abstract

We compare ground state properties of 3D Ising spin glasses with Gaussian couplings using results from off-equilibrium numerical simulations at non-zero (but low) temperatures. We find that the non-zero temperature properties of the system smoothly connect to the $T = 0$ behaviour, confirming the point of view that results established at $T = 0$ typically also give relevant information about the $T \neq 0$ physics of the system.

PACS numbers: 75.50.Lk, 64.60.Cn, 05.50.+q

1. Introduction

Spin glass physics is difficult, because it is complex to establish results that frequently go beyond the mean field level (see, for example, [1] and references therein), numerical simulations are the technique of choice (see, for example, [2] and references therein).

Recently, ground-state techniques have become popular (see, for example, [3] and references therein). The big advantage here is that one is (down in the broken phase) surely as far as possible from the critical temperature T_c. Our goal is to observe the effects of the $T = 0$ fixed point, and to remove spurious effects due to the critical point at $T = T_c$; these contaminations are minimized when working at $T = 0$. Also, the use of exact ground states solves the problem of thermalization, that is typically very severe on spin glasses at low values of T. The price one pays is that contacts with $T \neq 0$ physics are not clear; it could even be (but it does not seem to be so, and here we will show that this is not the case) that what happens at $T = 0$ is essentially different from what happens for even an infinitesimal value of the temperature.

Here, we will use a tool to further check the consistency of the $T = 0$ and the $T \neq 0$ phase spaces. Thanks to off-equilibrium dynamical simulations, we will be able to study large

lattice sizes and restricted sectors of the phase space; this will allow us to better show that $T = 0$ physics is compatible with the results one obtains at finite values of the temperature.

The second important part of this work is that, thanks to off-equilibrium dynamical numerical simulations, we are able to keep under control crucial observables such as overlap–overlap correlation functions and block overlaps. These observables are very important since they allow us to discriminate potentially misleading situations, such as those where interfaces induce a seemingly non-trivial overlap probability distribution $P(q)$ from a true replica symmetry breaking.

2. Model, algorithm and observables

We have simulated a three-dimensional (3D) Ising spin glass with Gaussian couplings on a cubic lattice with periodic boundary conditions. The Hamiltonian is

$$\mathcal{H} \equiv -\sum_{\langle i,j \rangle} \sigma_i J_{ij} \sigma_j \tag{1}$$

where the sum runs over all couples of nearest neighbours, the $\sigma_i = \pm 1$ are Ising spins and the couplings J_{ij} are quenched random Gaussian variables with zero mean and unit variance.

We have focused mainly on the measurements of two very important observables; they are both useful to distinguish situations where a true non-trivial behaviour of the probability distribution of the overlaps is present from situations where interfaces could present a misleading situation (because of finite size effects or even in the infinite volume limit, see the discussion in [4, 5] and references therein).

The first observable is an overlap, i.e. the measurements of how similar two typical configurations at equilibrium are. Here, we define the overlap only in a small part of the lattice: we compute the block overlap $q_{\mathcal{B}}$ on a $2 \times 2 \times 2$ cube (that we call a $\mathcal{B}$-cube, here with $\mathcal{B} = 2$):

$$q_{\mathcal{B}} = \frac{1}{\mathcal{B}^3} \sum_{i \in \mathcal{B}} q_i \tag{2}$$

with the usual site overlap

$$q_i \equiv \sigma_i \tau_i \tag{3}$$

where σ and τ are two independent equilibrium configurations of the system in the same realization of the quenched disorder. We call, as usual, q the total overlap computed on all the lattice, i.e. the average of the site overlap q_i over all lattice sites. In the following, we will, as usual, denote with brackets the thermal average for one given realization of the quenched disorder, $\langle(\cdot)\rangle$; by averaging at a given Monte Carlo time t, we will mean averaging over different realizations of the dynamical process, and we will indicate this average with $\langle(\cdot)\rangle_t$. We will denote with an over-line the average over the quenched disorder, $\overline{(\cdot)}$.

We have computed the full probability distribution $P_{\mathcal{B}}(q_{\mathcal{B}}, t, T)$ of the $\mathcal{B} = 2$ block overlap $q_{\mathcal{B}}$ as a function of temperature T and (Monte Carlo) time t of a so-called *off-equilibrium dynamics*. In an off-equilibrium numerical simulation (see, for example, [6]) we use a 'very large' lattice size, and work at values of the temperature low enough to make sure that the system is not thermalized; this is already true for medium-size lattices in the case of systems that are characterized by slow dynamics, as is the case here. In this situation, we work by extrapolating off-equilibrium, finite time measurements to infinite time. On the one hand, the advantage of the method is that we are basically free from finite size effects and, on the other

hand, we can learn additional information from the pattern of the approach to equilibrium (for example, in [6], this turns out to be a nice way to learn about the minimal value of the allowed overlap, $q_{\min}$). However, the disadvantage is that we have to rely on an extrapolation to infinite time, that can turn out to be not so trivial.

The second relevant observable is the overlap–overlap correlation function (defined on the full lattice) computed at distance $\boldsymbol{r}$, and defined as

$$C(\boldsymbol{r}, t, T) \equiv \overline{\langle q_i q_{i+r} \rangle_t}. \tag{4}$$

Here we will analyse only $C(1, t, T)$, since among all the different C for different $\boldsymbol{r}$ values, it is the one least affected by statistical errors.

In our working conditions, $C(\boldsymbol{r}, t, T)$ depends on the initial total overlap probability distribution $P(q, t = 0, T)$. In our case, since we have used very large lattice sizes and are starting from an average zero overlap (we start by evolving two independent, uncorrelated random configurations), and since we are limited to a number of Monte Carlo sweeps (of the full lattice) of the order of 10^7, we are not able to change away from zero the total overlap, and at least roughly we have that $P(q, t, T) \simeq P(q, t = 0, T)$. Because of that, the correlation functions we measure are very different from the equilibrium correlation functions, and can be written as

$$\begin{aligned} C(\boldsymbol{r}, t, T) &= \int \mathrm{d}q\, P(q, t, T) C(\boldsymbol{r}, t, T, q) \\ &\simeq \int \mathrm{d}q\, P(q, t = 0, T) C_0(\boldsymbol{r}, t, T, q) \end{aligned} \tag{5}$$

where by $C(\boldsymbol{r}, t, T, q)$ we denote the spatial correlation functions at time t and temperature T computed by including only couples of configurations having total overlap q, and by $C_0(\boldsymbol{r}, t, T, q)$ we denote the correlation functions computed with initial conditions $P(q, t = 0, T)$.

In the numerical simulations that we will discuss in the following, we have been starting from an initial probability distribution peaked around zero total overlap, i.e, our results are determined by the value of $C(\boldsymbol{r}, t, T, q = 0)$. In other terms, we are discussing here the dynamics of the $q = 0$ sector of the system (see [5] for further details). As we have stressed in the introduction, our main goal here is to relate numerical results computed from an off-equilibrium dynamics at non-zero temperature with equilibrium results obtained at zero temperature using techniques that give exact ground-state configurations on reasonable size lattices (see, for example, [7, 8]).

In recent studies, computing spin glass ground states, the technique of choice, was based on computing the so-called *mixed overlap*, i.e., the overlap computed between a ground state in a finite volume with periodic boundary conditions (pbc) in all directions and another ground state obtained by imposing anti-periodic boundary conditions (abc) in one direction and pbc in the other directions of the cubic lattice with the same realization of the quenched couplings J. In a theory with continuously broken replica symmetry [9] in the infinite volume limit, there are many ground states with total site overlap q and total *link overlap* q_l (that coincides with the correlation function C computed at distance 1) different from 1 [8]. In contrast, a droplet approach [10] implies a behaviour similar to that of the usual ferromagnet, where the link overlap (and the site overlap if we activate an infinitesimal magnetic field) go to 1 in the thermodynamical limit. Both [7] and [8] compute the $\mathcal{B} = 2$ block overlap.

Now a key remark is in order. The procedure we have just described to compute overlaps in the ground-state sector leads to the comparison, if the RSB picture holds, of ground states with $q = 0$ (changing the boundaries we favour ground states with small overlap); which

means that these results based on ground states describe the link overlap in the $q = 0$ sector of the system. This is the main reason for interest in these dynamical simulations; we are simulating here the $q = 0$ sector of the theory, and since we are working on very large lattice sizes we are sampling only this sector. In other words, when extrapolating our measurements of $C_\infty(1, T)$ (by the subscript ∞ we mean we have already extrapolated, hopefully and faithfully, to $t = \infty$) from our low values of the temperature T down to $T = 0$ we should find, if the RSB picture is consistent, the same results found in the direct analysis of the ground states.

We will also try to check the behaviour of a different relevant observable. In [8], the authors have computed the probability that, for example, a $\mathcal{B} = 2$ block does not intersect an interface: one can relate this probability to the probability of finding that a $\mathcal{B} = 2$ block is ± 1. Again our strategy will be to compute the probability of this event at non-zero temperatures and to extrapolate the result down to $T = 0$.

A very direct relation about the second moment of the ($\mathcal{B} = 2$) block overlap and the q–q correlation function (4) can be established by noticing that

$$\left\langle q_{\mathcal{B}}^2 \right\rangle (t, T) = \tfrac{1}{8}[C(0, t, T) + 3C(1, t, T) + 3C(\sqrt{2}, t, T) + C(\sqrt{3}, t, T)]. \quad (6)$$

3. Numerical results

Our numerical simulations have been run on a APE100 parallel supercomputer [11]; on the more powerful version of the computer (the so-called 'tower' version) our Monte Carlo code for simulating 3D Ising spin glasses with Gaussian couplings has a peak performance of 5 GF.

For all the numerical simulations described in this paper, we have averaged our data on four different realizations of the random quenched disorder. In each disorder realization, we have simulated two independent copies of the system (useful to compute the different overlaps, block overlaps and correlation functions). We have used a straightforward metropolis algorithm. We have used a lattice of linear size $L = 64$ and volume $V = L^3 = 2^{18}$.

We have analysed two kind of runs. 'Short' runs have been used to compute the extrapolated value of the overlap–overlap correlation function. In these short runs, we have simulated temperatures $T = 0.9,\ 0.8, 0.7, 0.6, 0.5, 0.4, 0.35$ and 0.3 during 819 200 Monte Carlo steps. We have presented a preliminary and partial analysis of some of these data in [14] (only for $T \geqslant 0.35$ and only as far as the dependence of the critical exponents over temperature is concerned; we had not analysed, for example, the prefactors, which are very relevant to the physics studied in this paper (see below).

We use a simple scheme in the 'short' runs. We start from two initial independent random configurations, and suddenly start iterating at the working temperature well below the critical one: $T < T_c$ ($T = 0.9, 0.8, 0.7, 0.6, 0.5, 0.4, 0.35$ or 0.3). At each T value we will eventually extrapolate to infinite time to get a T-dependent asymptotic value, that we will, in turn, try and extrapolate down to $T = 0$.

In order to compute the dynamical behaviour of the block overlap, we have used 'long' runs. Here, we have used the previous scheme for four values of the temperature, $T = 0.7, 0.6, 0.5$ and 0.35, with 6553 600 Monte Carlo updates of the full lattice performed at each value of T.

In the 'short' runs, we measure the time-dependent observables on logarithmic time scales: i.e., at times $t = 100, 200, 400, 800, \ldots$. In the 'long' runs, we measure every 32 768 steps.

In the next two subsections, we will discuss separately our numerical results for the correlation functions and for the window overlap.

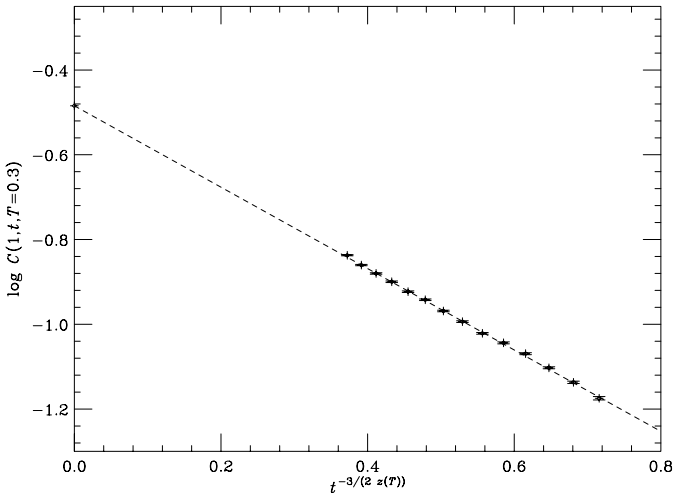

Figure 1. Values of $C(1, t, T)$ at $T = 0.3$ (the lowest value of T that we use) versus $t^{-3/(2z)}$. We also show our best fit to form (10).

3.1. Correlation functions

In this section, we will always indicate by $C(1, t, T)$ the $q = 0$ component of the overlap–overlap correlation function, i.e., $C(r = 1, t, T, q = 0)$, that, as we have discussed in detail in section 2, is the quantity we are measuring.

The dependence of $C(1, t, T)$ on time can be expressed through knowledge of the dynamical critical exponent $z(T)$ (that depends on T). We have that

$$C(1, t, T) = f\left(t^{\frac{1}{z(T)}}, T\right).$$

From numerical simulations [12–16] (that are in very good agreement with real experiments here [17]) we know that

$$z(T) = \frac{1}{T}(6.2 \pm 0.3). \tag{7}$$

Another useful piece of information [14–16] is that

$$C(x, t, T) \propto \frac{1}{\sqrt{x}} \exp\left[-\left(\frac{x}{\xi(t, T)}\right)^{3/2}\right] \tag{8}$$

where $\xi(T) \propto t^{1/z(T)}$ is the time-dependent *dynamical correlation length* of the system. Because of that we expect that

$$\log C(1, t, T) \simeq a(T) + b(T)t^{-3/(2z(T))} \tag{9}$$

asymptotically for large times. As t diverges, $C(1, t, T)$ tends to the constant value $\exp(a(T)t)$, that we have called the prefactor in the previous section.

In figure 1, we show the extrapolation of $C(1, t)$ to $t = \infty$ for the lowest temperature we use, $T = 0.3$ (this is the most difficult extrapolation, and fits at larger T values are easier). The dashed line is for the best fit to the form

$$\log C(1, t, T) = a(T) + b(T)t^{-c(T)}. \tag{10}$$

The fit is good and the extrapolation looks reasonably safe. By this kind of fit, we are able to obtain reliable extrapolated values for all the values of T we study, that we show in figure 2

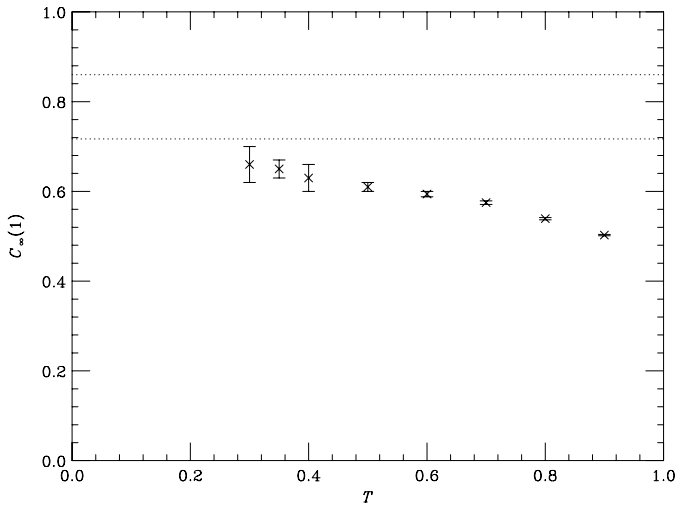

Figure 2. Values extrapolated to infinite time of the correlation function at distance $d = 1$, $C_\infty(1, T)$, versus T. We have also marked by two horizontal dotted lines the interval where the value computed in [8] using $T = 0$ ground state calculations lies. The consistency of the two results is clear.

versus the temperature T. We have checked that the value of $c(T)$ of the best fit to the form 10 is in very good agreement (i.e., inside the margins suggested by the estimated statistical error) with the value of $3/(2z(T))$. The discrepancies between the extrapolated value obtained by using a three- or two-parameter fit (i.e., by fixing $c(T)$ to $3/(2z(T))$ in equation (10) or by letting it free) are within the statistical errors.

For a detailed numerical study of the functional form suggested in equation (10), see [14–16]. An exhaustive analysis of the correlation functions computed at zero total overlap has been performed in three [14–16], four [18] and six dimensions [19]; in all cases the system turns out to have a very similar behaviour, independent of the spatial dimensionality. In six dimensions, the agreement with the quantitative analytical predictions obtained by De Dominicis *et al* [20] is very good [19].

In the same figure, we have also plotted the statistical interval allowed for the value of the link overlap at $T = 0$ from ground state calculations (see [8]). The statistical error in our values of $C_\infty(1, T)$ grows when T decreases, but in the limit given by these errors the $T = 0$ result and a reasonable extrapolation of the finite T results obtained here look completely consistent.

The interval we have drawn in the figure is 0.79 ± 0.07 and we have computed it by looking at the data from [8]. We have used the four different (but statistically compatible) values obtained there for q_l. By extrapolating q_l for $L \to \infty$, one obtains $q_l = 0.755 \pm 0.015$ or $q_l = 0.80 \pm 0.06$ using a linear or a quadratic fit in $1/L$, respectively. By studying correlation function [8], one also obtains $C(1) = 0.732 \pm 0.008$ (for the transverse correlation) and $C(1) = 0.722 \pm 0.005$ (for the perpendicular correlation). Taking into account all these figures, we have obtained the confidence interval (at one standard deviation) for the link overlap that we were quoting before.

3.2. Block overlaps

Our second set of measurements concerns the so-called *block overlap* (that we also call *window overlap* or *box overlap*, and have been computed on a $\mathcal{B} \times \mathcal{B} \times \mathcal{B} = 2 \times 2 \times 2$ box). As in

the case of correlation functions, we start from two independent random configurations, and cool them down according to the annealing schedule we have described before (using what we have called the 'long' runs). During these runs, we have computed the full probability distribution of the window overlap at different times t.

In this section, our main goal is to compute $P_{\mathcal{B}}(\pm 1)$, i.e., the value (extrapolated to infinite time first and $T = 0$ later) of the probability that a $\mathcal{B}$ block has an overlap of maximal modulus. To simplify the notation, from now on we will be working with a symmetrized overlap probability distribution, i.e., we will consider $P_{\mathcal{B}}(|q|, t, T)$, that can have support in $(0, 1)$; this object is interesting because it is exactly the probability that the interface between different phases does not intersect with a cube of size 2. As we have already discussed, this probability has been computed in [8] at $T = 0$, and we will try here to connect these results with the $T \neq 0$ physics.

The main result of [8] is that, at $T = 0$ and in the limit of the lattice size $L \longrightarrow \infty$

$$P_1(\mathcal{R}) \simeq 0.65 \pm 0.05. \tag{11}$$

Our working ansatz for the time dependence of $P_{\mathcal{B}}(|q| = 1)$ has been, as we will justify now, that

$$\log P_{\mathcal{B}}(|q| = 1, t, T) = \log P_{\mathcal{B}}^{t=\infty}(|q| = 1, T) + \frac{a(T)}{t^{3/(2z(T))}} \tag{12}$$

and we have used $z(T) = \frac{6.2}{T}$.

Let us see why things work in this way. From equation (6), we know that $\langle q^2 \rangle_B$ scales as an overlap–overlap correlation function. But for large times and for distances such that $x \ll t^{1/z}$, equation (8) tells us that the correlation function behaves as

$$C(x, t) \propto \frac{1}{\sqrt{x}} \left[1 - A \frac{x}{t^{3/(2z(T))}} \right] \tag{13}$$

where A is a suitable constant. This implies in turn that

$$\left\langle q_{\mathcal{B}}^2 \right\rangle (t, T) \simeq a(T) + \frac{b(T)}{t^{3/(2z(T))}} \tag{14}$$

where $a(T)$ and $b(T)$ are constants that depend only on T. Now, since

$$\left\langle q_{\mathcal{B}}^2 \right\rangle (t, T) \equiv \int_{-1}^{1} \mathrm{d}q \, P_{\mathcal{B}}(q, t, T) q^2 \tag{15}$$

if we define $\Delta P_{\mathcal{B}}(q, t, T) \equiv P_{\mathcal{B}}(q, t, T) - P_{\mathcal{B}}^{t=\infty}(q, T)$, it is clear that

$$\int_{-1}^{1} \mathrm{d}q \, \Delta P_{\mathcal{B}}(q, t, T) q^2 \simeq \frac{b(T)}{t^{3/(2z(T))}}. \tag{16}$$

Things are more clear if we write equation (16) for discrete values of $q_{\mathcal{B}}$ (that is what happens for finite $\mathcal{B}$):

$$\sum_{q<1} \Delta P_{\mathcal{B}}(q, t, T) q^2 + \Delta P_{\mathcal{B}}(q = 1, t, T) = \frac{b(T)}{t^{3/(2z(T))}}. \tag{17}$$

If we assume that all the components with $q > 0$ scale in the same way, this shows that

$$\Delta P_{\mathcal{B}}(q = 1, t, T) \equiv P_{\mathcal{B}}(q = 1, t, T) - P_{\mathcal{B}}^{t=\infty}(q = 1, T) \simeq t^{-3/(2z(T))} \tag{18}$$

and so,

$$P_{\mathcal{B}}(|q| = 1, t, T) = P_{\mathcal{B}}^{t=\infty}(|q| = 1, T) + \frac{d(T)}{t^{3/(2z(T))}} \tag{19}$$

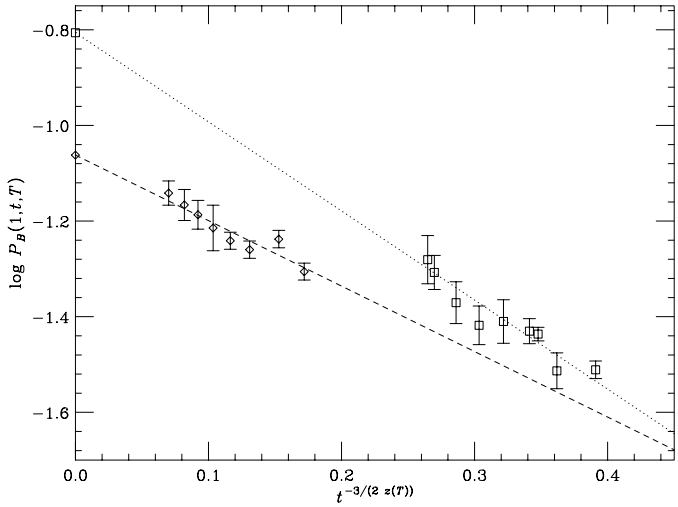

Figure 3. $\mathrm{Log}P_{\mathcal{B}}(1, t, T)$ versus $t^{-\frac{3}{2z(T)}}$ for $T = 0.7$ (diamonds) and $T = 0.35$ (squares). The dashed line (dotted line) is for the best fit to ansatz (12) for $T = 0.7$ ($T = 0.35$, respectively).

and we recover (12) by taking logs in (19). We have used (12) instead of (19) since we have (slightly) better scaling even for small times. We have checked that both kinds of fits provide us with compatible values of $P_{\mathcal{B}}^{t=\infty}(|q| = 1, T)$.

We will use equation (12) to fit the values of $P_{\mathcal{B}}^{t=\infty}(q = 1, T)$ at different temperatures. Our argument says nothing about the behaviour of $\Delta P_{\mathcal{B}}(q = 0, t, T)$, while $\Delta P_{\mathcal{B}}(q, t, T)$ for $q \neq 0$ follows the same scaling law valid for $\Delta P_{\mathcal{B}}(q = 1, t, T)$.

We have checked that our numerical data are well fitted by the behaviour of equation (12). We show two plots, corresponding to two different temperatures: $T = 0.7$ and $T = 0.35$, in figure 3. In the plots, we also draw our best fits to ansatz 12.

The fit of figure 3 for $T = 0.7$, for example, looks reasonably reliable. $P_{\mathcal{B}}$ depends very slowly on T, and our numerical data have as support a range of times as large as the range we need to extrapolate through. In contrast, the fit of (3) for $T = 0.35$ (again, the one at our lowest T value, i.e., our most difficult fit) looks less happy even if one did not expect very strange things to happen; since $\frac{1}{z(T)}$ at such low T is becoming very small, our data vary on a small support, and the $t = \infty$ point looks far away. The very large error that appears in figure 4 is an effect of this phenomenon.

In figure 4, we show the values of $P_{\mathcal{B}}^{t=\infty}(q = 1, T)$ extrapolated up to $t = \infty$ versus T. Because it is difficult to get precise results at low T values, the evidence we have established is not very strong; still, figure 4 clearly shows that our present low T results are completely compatible with the $T = 0$ results.

We end this section by performing a last consistency check. We compare the values of $\langle q_{\mathcal{B}}^2 \rangle$ with the values of the correlation function (in both cases extrapolated to infinite time). Using equation (8), we can write equation (6) as

$$\langle q_{\mathcal{B}}^2 \rangle (T) = 0.125 + 0.785 C_{\infty}(1, T). \tag{20}$$

In table 1, we show the values of $\langle q_{\mathcal{B}}^2 \rangle (T)$ obtained by direct measurements of $q_{\mathcal{B}}$ and the value obtained by summing up correlation functions, according to the right-hand side of equation (20): the agreement of the two quantities is very reasonable at all T values. The values of $\langle q_{\mathcal{B}}^2 \rangle (T)$ have been extrapolated at infinite time by using equation (14).

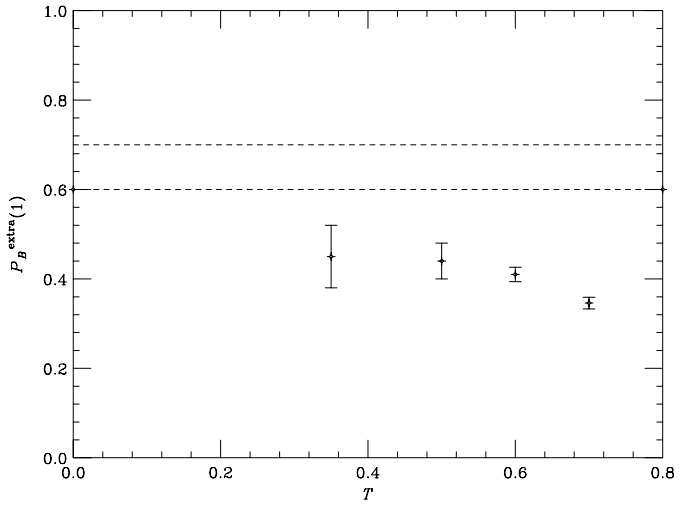

Figure 4. $P_{\mathcal{B}}^{t=\infty}(1, T)$ versus T. The horizontal line corresponds to the confidence limit obtained in ground state computations.

Table 1. Test of relation (20).

T	$\langle q_{\mathcal{B}}^2 \rangle(T)$	rhs of equation (20)
0.7	0.585 ± 0.002	0.576 ± 0.004
0.6	0.596 ± 0.009	0.594 ± 0.004
0.5	0.57 ± 0.02	0.60 ± 0.01
0.35	0.61 ± 0.03	0.64 ± 0.02

4. Conclusions

The results of our investigation are indeed positive. Physical observables computed at $T = 0$ are compatible with values computed on large lattices, thanks to an off-equilibrium dynamics, and extrapolated from measurements at low and finite T. Our observables of choice are interesting observables, since they not only show that our system has a non-trivial $P(q)$, but also that this non-trivial $P(q)$ is the *bona fide* effect of replica symmetry breaking, and not the effect of some fancy kind of interface.

We have been able to use very low T values, while still keeping good control over $t \to \infty$ fits. When we lower T and eventually $T \longrightarrow 0$, the data collapse, in reasonable accuracy given by the large statistical error, to the $T = 0$ results. It is important to remark, also as far as planning future, more precise studies is concerned, that it is really very difficult to run accurate numerical simulations in the region $T \leqslant 0.3$ with the computers available nowadays (for example at $T = 0.1$, the dynamical critical exponent is of the order of 60).

Acknowledgment

JJRL acknowledges partial financial support from CICyT (PB98-0842).

References

[1] Binder K and Young A P 1986 *Rev. Mod. Phys.* **58** 801
Mézard M, Parisi G and Virasoro M A 1987 *Spin Glass Theory and Beyond* (Singapore: World Scientific)
Fisher K H and Hertz J A 1991 *Spin Glasses* (Cambridge: Cambridge University Press)
Young A P (ed) 1998 *Spin Glasses and Random Fields* (Singapore: World Scientific)

[2] Marinari E, Parisi G and Ruiz-Lorenzo J J 1998 Numerical simulations of spin glass systems *Spin Glasses and Random Fields* ed A P Young (Singapore: World Scientific)

[3] Rieger H 1998 *Frustrated Systems: Ground State Properties via Combinatorial Optimization (Lecture Notes in Physics vol 501)* (Heidelberg: Springer)

[4] Marinari E, Parisi G, Ricci-Tersenghi F and Ruiz-Lorenzo J J 1998 *J. Phys. A: Math. Gen.* **31** L481

[5] Marinari E, Parisi G, Ricci-Tersenghi F, Ruiz-Lorenzo J and Zuliani F 2000 *J. Stat. Phys.* **98** 973

[6] Marinari E, Parisi G and Zuliani F 1998 *J. Phys. A: Math. Gen.* **31** 1181
Parisi G, Ricci-Tersenghi F and Ruiz-Lorenzo J J 1998 *Phys. Rev.* B **57** 13617

[7] Palassini M and Young A P 1999 *Phys. Rev. Lett.* **83** 5126
Palassini M and Young A P 2000 *Preprint* cond-mat/0004485

[8] Marinari E and Parisi G 2000 *Phys. Rev.* B **62** 11677 (*Preprint* cond-mat/0005047)
Marinari E and Parisi G 2000 *Preprint* cond-mat/0002457
Marinari E and Parisi G 2000 *Preprint* cond-mat/0007493

[9] Parisi G 1979 *Phys. Lett.* A **73** 203
Parisi G 1980 *J. Phys. A: Math. Gen.* **13** L115
Parisi G 1980 *J. Phys. A: Math. Gen.* **13** 1101
Parisi G 1980 *J. Phys. A: Math. Gen.* **13** 1887

[10] McMillan W L 1984 *J. Phys. C: Solid State Phys.* **17** 3179
Bray A J and Moore M A 1986 *Heidelberg Colloquium on Glassy Dynamics* ed J L Van Hemmen and I Morgenstern (Heidelberg: Springer) p 121
Fisher D S and Huse D A 1986 *Phys. Rev. Lett.* **56** 1601
Fisher D S and Huse D A 1988 *Phys. Rev.* B **38** 386

[11] Battista C *et al* 1993 *Int. J. High Speed Comput.* **5** 637

[12] Rieger H 1995 *Annual Reviews of Computational Physics II* (Singapore: World Scientific) p 295

[13] Kisker J, Santen L, Schreckenberg M and Rieger H 1996 *Phys. Rev.* B **53** 6418

[14] Marinari E, Parisi G, Ricci-Tersenghi F and Ruiz-Lorenzo J J 2000 *J. Phys. A: Math. Gen.* **33** 2373

[15] Marinari E, Parisi G and Ruiz-Lorenzo J J 1998 *Phys. Rev.* B **58** 14852

[16] Marinari E, Parisi G, Ritort F and Ruiz-Lorenzo J J 1996 *Phys. Rev. Lett.* **76** 843

[17] Joh Y G, Orbach R, Wood G G, Hammann J and Vincent E 1999 *Phys. Rev. Lett.* **82** 438

[18] Parisi G, Ricci-Tersenghi F and Ruiz-Lorenzo J J 1996 *J. Phys. A: Math. Gen.* **29** 7943

[19] Parisi G, Ranieri P, Ricci-Tersenghi F and Ruiz-Lorenzo J J 1997 *J. Phys. A: Math. Gen.* **30** 7115

[20] De Dominicis C, Kondor I and Temesvari T 1998 Beyond the Sherrington–Kirkpatrick model *Spin Glasses and Random Fields* ed P Young (Singapore: World Scientific)